11th World Congress on Structural and Multidisciplinary Optimisation
07th -12th, June 2015, Sydney Australia

Optimization of bone tissue scaffolds fabricated by robocasting technique

Ali Entezari[1], Zhongpu Zhang[2], Junning Chen[3], Qing Li[4]

[1]School of Aerospace, Mechanical and Mechatronic Engineering, University of Sydney, NSW, Australia, aent9923@uni.sydney.edu.au
[2]School of Aerospace, Mechanical and Mechatronic Engineering, University of Sydney, NSW, Australia, leo.zhang@sydney.edu.au
[3]School of Aerospace, Mechanical and Mechatronic Engineering, University of Sydney, NSW, Australia, jche8767@uni.sydney.edu.au
[4]School of Aerospace, Mechanical and Mechatronic Engineering, University of Sydney, NSW, Australia, qing.li@sydney.edu.au

1. Abstract
While excellent biological and mechanical properties of ceramic scaffolds place them amongst the main candidates for applications of bone and cartilage repair, an optimum trade-off between critical biological and mechanical functions remains challenging during design process. These ceramic scaffolds should not only enhance tissue regeneration function, but also be of adequate mechanical strength particularly in load-bearing applications. One of the techniques used for the fabrication of ceramic scaffolds is robocating which has so far received little attention in the currently available optimization analyses related to the design of these scaffolds. In this study a vigorous optimization analysis based on finite element (FE) method is performed to maximize compressive strengths of such scaffolds while maintaining the minimum biological functions required for tissue ingrowth. The results demonstrate that an optimized functionality of ceramic scaffolds fabricated by robocasting needs a careful design of critical geometrical features.
2. Keywords: Robocasting, bone tissue engineering, ceramic scaffolds, optimization

3. Introduction
Today, there is an increasing need for the treatment of bone defects caused by trauma, infection, or injuries. Current treatments for bone defects include autografts, allografts and other synthetic substitutes such as metals and bio-ceramics [1] which all have their own problems and limitations. As a result, recent research has been devoted to bone tissue engineering (BTE) which emerged in the early 1990s to address limitations of tissue grafting [2]. In the scaffold tissue engineering strategy, a 3D scaffold populated with cells and signaling molecules is used to provide temporary biomechanical environment for tissue regeneration for promoting cell attachment and growth of neo-tissue. Despite remarkable progress in BTE, many challenges and limitations still exist on the way of such scaffolds to be marketed and replace current conventional treatments of bone defects. One of the most important challenges associated with BTE scaffolds is to optimize their mechanical and biological functionality so that they can provide adequate mechanical support and enhance tissue regeneration. These two functions often result in conflicting design goals, because improved mechanical support function needs a dense scaffold while enhanced tissue regeneration function requires a porous scaffold. Therefore, an optimum trade-off between biological and mechanical criteria is necessary in the design of bone scaffolds.
A number of different optimization studies based on numerical methods have been established in literature [3, 4]. Hollister and colleagues [5] were amongst the first who applied the finite element based homogenization theory to relate periodic orthogonal pore diameters of a scaffold to its effective stiffness and porosity. They used topology optimization approach to matching the effective moduli of minipig mandibular cancellous bone to ceramic material. In other studies, the direct homogenization [6] and inverse homogenization approaches [7] were implemented to maximize the effective modulus of BTE scaffolds. Further studies were performed by Chen et al. [8] and Adachi et al. [9], in which the interaction process of scaffold degradation and tissue regeneration were also taken into account in the optimization process.
While significant advances have been made in available optimization studies on tissue engineering scaffolds, almost none of these studies have considered fabrication limitations induced by the so-called robocasting technique. Another concern associated with currently available optimization studies is that they do not take account of scaffold's strength as a design criterion in the optimization process because stress is a non-differentiatable quantity [10, 11] which could have significantly limited the reliability of such optimization approaches. Therefore consideration of fracture strength is critical to develop more trustworthy optimization methods, particularly for ceramic scaffolds whose application in load-bearing scenarios is often limited due to the inherent brittleness and relatively low fracture strength. Numerical methods have shown their capability to effectively predict fracture strength of such scaffolds based on the stress fields obtained by FE simulations [12].

In this study, FE method will be used to conduct a design optimization analysis of Hydroxyapatite (HA) scaffolds fabricated by robocasting technique to maximize their strength for load-bearing applications.

4. Method

Different parameters such as porosity, pore size, and interconnectivity of scaffolds affect the quality of tissue regeneration, among which porosity is the main design variable known to influence tissue regeneration [13], which has often been considered as a biological design criterion in different optimization studies. Here, while a constraint is imposed on the porosity of scaffolds in order to satisfy biological functions, the effect of different geometrical features will be investigated on strength and effective modulus of the scaffolds. Since the scaffolds are assumed to be fabricated by the robocasting technique, fabrication limitations related to this technique should be taken into account. Robocasting or direct ink writing (DIW) technique is a solid free form (SFF) fabrication method in which a filament of ink is extruded from a nozzle in a layer-wise fashion and ultimately forms a 3-D mesh of interpenetrating struts whose structure can have different patterns depending on design requirements [14]. Figure 1 shows three of most common patterns fabricated by this technique.

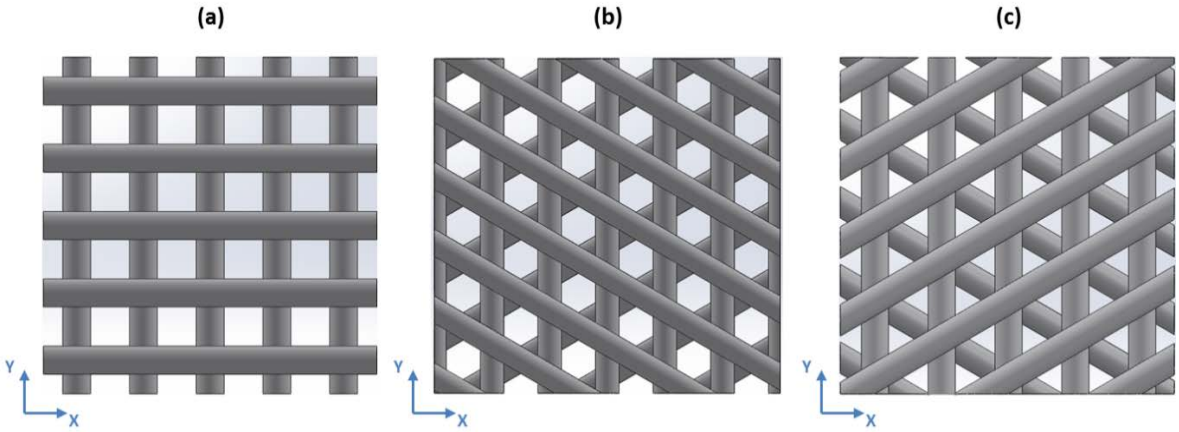

Figure 1 : Three of most common patterns fabricated by robocasting technique; (a) square pattern; (b) honey comb pattern; (c) triangle pattern

In the first step, a comparison will be made between the fracture strengths related to each of the above patterns. For this purpose, three different scaffolds based on these patterns are created in SolidWorks software. All three scaffolds have similar porosity, strut and pore size. Then FE simulations are carried out using ABAQUS/CAE software in which the scaffolds are placed in between two parallel analytical rigid plates. One of the rigid plates is fixed while the other can move under the action of a linearly increasing applied force. The force is applied perpendicular to the printing plane (x-y plane) simulating a compression test in the z direction. Fracture strength for each test is predicted based on a critical stress criterion by assuming an opening fracture mode (mode I), which is the most commonly activated in brittle materials [15]. This fracture mode is known to induce cracking perpendicular to the rod axes over the entire structure at the points experiencing the highest tensile stress (σ_t) [12]. Hence, in the current analyses, fracture is presumed to occur when the maximum of σ_t in the structure equals the inert fracture strength (σ_f) of the rods reported in [12]. For instance, Figure 2 represents FE stress contours corresponding to the highest range of tensile stress in the square pattern. Since an applied compressive stress of 39 (MPa) on the top surface leads to the maximum tensile stress equivalent to σ_f in the structure, it will be taken as the compressive strength of the scaffold. For the determination of the maximum of tensile stress, stress at near-contact regions and singularities are ignored. Intrinsic mechanical properties of HA [12] used in current numerical simulations have been given in Table 1.

Table 1 : Intrinsic mechanical properties of HA

	E (GPa)	υ	σ_f (MPa)
Hydroxyapatite (HA)	85	0.28	80

Table 2 represents the mechanical properties related to the three different configurations of tissue scaffolds obtained by FE analysis.

Table 2 : Mechanical properties for the three different configurations of scaffolds

	Square pattern	Honey comb pattern	Triangle pattern
Compressive strength (MPa)	39	6.5	33.8
Compressive effective modulus (GPa)	11.7	4.08	11.7

The results show that square pattern offers the highest compressive strength compared with the other two topologies. Another fact that can be concluded from the above results is that effective modulus of scaffolds may not be correlated to their strength, because as it can be observed, while square and triangle patterns have similar effective modulus, their strengths are not the same. Moreover, honey comb pattern offers an effective modulus which is almost three times less than the one related to square pattern, nevertheless, its strength is more than 6 times smaller than the one for square array. All these results signify the importance of considering strength as an optimization criterion for the design of bone tissue engineering scaffolds.

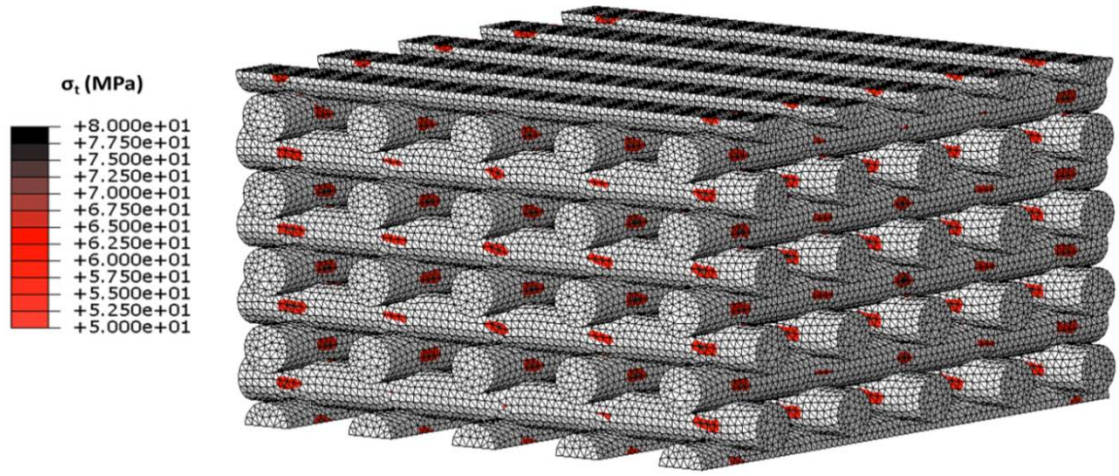

Figure 2 : FE stress contours corresponding to the highest range of tensile stress in the square pattern when a compressive stress of 39 MPa is applied perpendicular to the top surface (note that the stress contour shows only the top range of tensile stresses and the rest in grey indicates the lower stress)

Since it was observed that the square pattern offers better mechanical properties, the geometry of this pattern will be optimized as follows. In order to define controllable geometrical features, a representative volume element (RVE) whose repetition forms the entire scaffold needs to be defined. A RVE can often be found within scaffolds fabricated by the robocasting technique. Figure 3a clearly shows how the repetition of a RVE forms a scaffold with a square pattern.

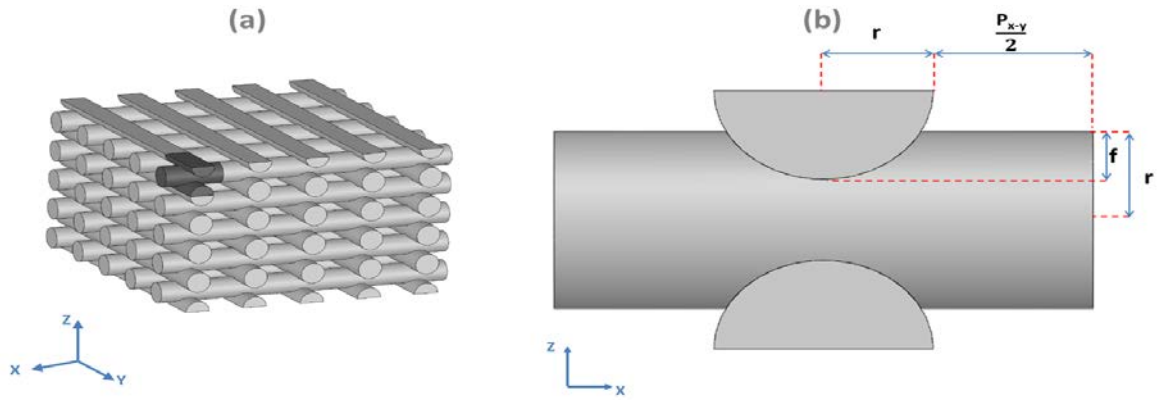

Figure 3 : A scaffold with square array fabricated by the robocasting technique; (a) the scaffold and a section displayed in black color represents a RVE within the scaffold; (b) controllable geometrical features in a RVE

Once a RVE is extracted from the scaffold, its geometrical features can be defined in terms of three controllable parameters as shown in Figure 3b. These parameters include scaffold's pore size in the printing plane ($P_{x\text{-}y}$), radius of each strut's cross section (r), and overlapping depth of two struts at top of one another (f). Given that the RVE is used to represent the entire scaffold, the porosity of scaffold can be expressed as:

$$Porosity = 100 \times \left[1 - \frac{2\pi r^2 (p_{x-y} + 2r) - 2V_f}{(4r - 2f)(p_{x-y} + 2r)^2} \right] \quad (1)$$

where V_f represents the intersection volume of two overlapping struts at top of one another, expressed as:

$$V_f = 4 \int_{r-f}^{r} \int_{0}^{\sqrt{r^2 - x^2}} \int_{0}^{\sqrt{r^2 - (2r - f - x)^2}} dz dy dx \quad (2)$$

Given that a desirable minimum value is required for porosity in order to satisfy tissue ingrowth function, the effect of other geometrical features on the strength and effective modulus of scaffolds can be investigated. It is obvious that at least two of the aforementioned geometrical features must change simultaneously, in order to maintain a constant desirable porosity of the scaffold. In this study a constraint is imposed on the porosity of scaffold (porosity = 60%), and 8 scaffolds with similar strut's radius (r) but different pore size ($P_{x\text{-}y}$) and overlapping depth (f) will be compared. Ratio of overlapping depth to radius (f/r), which can be easily adjusted during fabrication process by changing layer spacing, has a range from 10% to 80% in this study [16, 17]. The details of geometrical features related to these 8 scaffolds are given in Table 3.

Table 3 : Details of geometrical features related to 8 different scaffolds

	f/r	$\boldsymbol{P_{x\text{-}y}}$ (μm)	***f*** (μm)	Porosity
Scaffold 1	0.1	1140	30	60%
Scaffold 2	0.2	1080	60	60%
Scaffold 3	0.3	1020	90	60%
Scaffold 4	0.4	960	120	60%
Scaffold 5	0.5	900	150	60%
Scaffold 6	0.6	840	180	60%
Scaffold 7	0.7	780	210	60%
Scaffold 8	0.8	720	250	60%

5. Results and discussion

Figure 4 draws a comparison between compressive strengths related to these 8 different scaffolds with varying pore sizes ($P_{x\text{-}y}$) and overlapping depths (f) listed in Table 3. While a constant porosity is maintained for all scaffolds, a change in their controllable geometrical features can result in significant improvement of their compressive strength. It was observed that the optimum ratio of f/r for the geometry of such scaffolds is around 0.4. In fact, this optimized geometry could enhance the compressive strength by 32% and 17% compared with the cases in which f/r was 0.1 and 0.8 respectively.

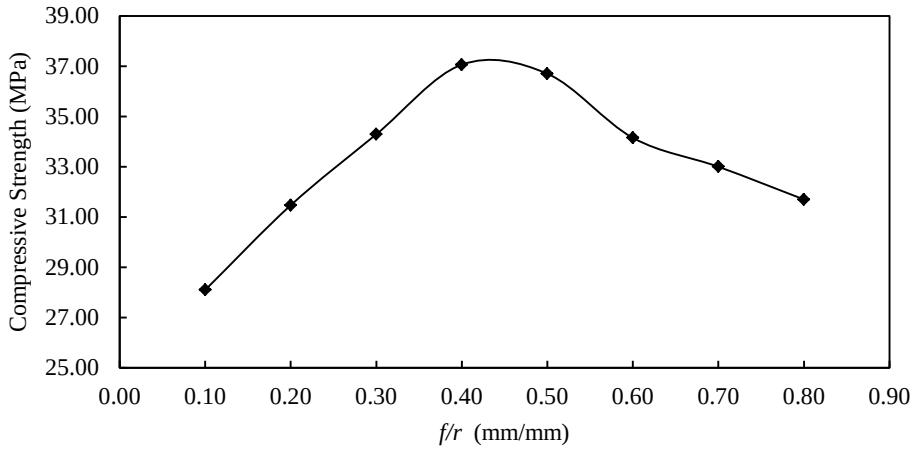

Figure 4 : Comparison between compressive strengths related to scaffolds with different f/r ratio

Since effective modulus of bone tissue engineering scaffolds plays an important role on their biomechanical functions, a comparison is also drawn between the compressive effective modulus related to these 8 scaffolds, which is presented in Figure 5. The results demonstrate that the optimized geometry will possess a greater effective modulus as well. Interestingly, it was observed that effective modulus for the optimized geometry (*f/r* = 0.4) was enhanced by 52% compared with the worst case (*f/r* = 0.1), whereas this improvement was only 32% for the compressive strength, a fact that shows it is important to take into the account the mechanical strength of scaffolds in the design optimization of bone tissue engineering scaffolds.

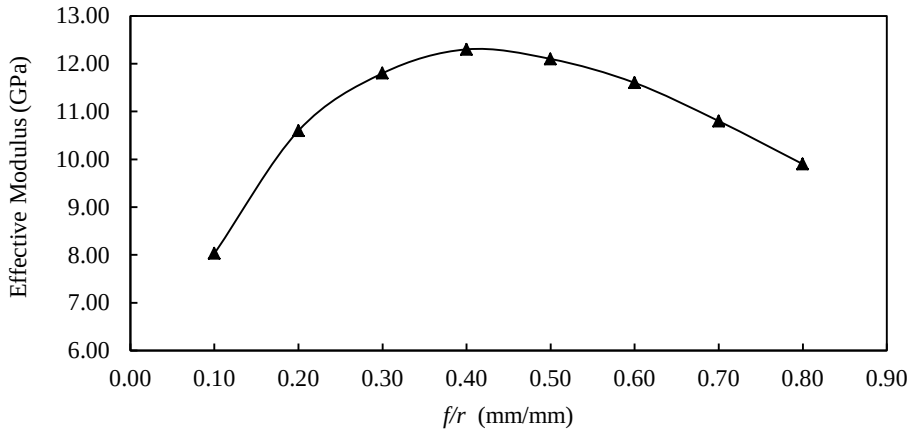

Figure 5 : Comparison between effective modulus related to scaffolds with different *f/r* ratio

6. Conclusion

This article could provide valuable insight into the optimization of ceramic scaffolds for bone tissue engineering applications fabricated by the robocasting technique. The results demonstrated that an optimized functionality of such scaffolds needs a careful control over particular geometrical features during design process. The square patterns showed better mechanical properties in terms of compressive strength compared with honey comb and triangular patterns. Moreover, for a square pattern, the results confirmed that an optimum relationship exists between its geometrical features which would significantly increase the compressive strength of such scaffolds while a constraint is imposed on its total porosity. It was also observed that effective modulus of scaffolds may not always represent their strength, a fact that signifies the importance of fracture strength to be considered as a design criterion in optimizations analyses of scaffolds.

7. References

[1] Goldberg, V.M., *Natural history of autografts and allografts,* in *Bone implant grafting*. 1992, Springer. p. 9-12.

[2] Moore, W.R., S.E. Graves, and G.I. Bain, *Synthetic bone graft substitutes.* ANZ journal of surgery, 2001. **71**(6): p. 354-361.

[3] Chan, K.S., et al., *A multiscale modeling approach to scaffold design and property prediction.* Journal of the Mechanical Behavior of Biomedical Materials, 2010. **3**(8): p. 584-593.

[4] van Cleynenbreugel, T., et al., *Trabecular bone scaffolding using a biomimetic approach.* Journal of Materials Science: Materials in Medicine, 2002. **13**(12): p. 1245-1249.

[5] Hollister, S., R. Maddox, and J. Taboas, *Optimal design and fabrication of scaffolds to mimic tissue properties and satisfy biological constraints.* Biomaterials, 2002. **23**(20): p. 4095-4103.

[6] Lin, C.Y., N. Kikuchi, and S.J. Hollister, *A novel method for biomaterial scaffold internal architecture design to match bone elastic properties with desired porosity.* Journal of Biomechanics, 2004. **37**(5): p. 623-636.

[7] Hollister, S.J. and C.Y. Lin, *Computational design of tissue engineering scaffolds.* Computer Methods in Applied Mechanics and Engineering, 2007. **196**(31–32): p. 2991-2998.

[8] Chen, Y., S. Zhou, and Q. Li, *Microstructure design of biodegradable scaffold and its effect on tissue regeneration.* Biomaterials, 2011. **32**(22): p. 5003-5014.

[9] Cahill, S., S. Lohfeld, and P. McHugh, *Finite element predictions compared to experimental results for the effective modulus of bone tissue engineering scaffolds fabricated by selective laser sintering.* Journal of Materials Science: Materials in Medicine, 2009. **20**(6): p. 1255-1262.

[10] Steven, G.P., Q. Li, and Y.M. Xie, *Multicriteria optimization that minimizes maximum stress and maximizes stiffness.* Computers & Structures, 2002. **80**(27–30): p. 2433-2448.
[11] Li, Q., G.P. Steven, and Y. Xie, *Evolutionary structural optimization for stress minimization problems by discrete thickness design.* Computers & Structures, 2000. **78**(6): p. 769-780.
[12] Miranda, P., A. Pajares, and F. Guiberteau, *Finite element modeling as a tool for predicting the fracture behavior of robocast scaffolds.* Acta biomaterialia, 2008. **4**(6): p. 1715-1724.
[13] Mikos, A.G., et al., *Prevascularization of porous biodegradable polymers.* Biotechnology and Bioengineering, 1993. **42**(6): p. 716-723.
[14] Stuecker, J.N., et al., *Advanced support structures for enhanced catalytic activity.* Industrial & engineering chemistry research, 2004. **43**(1): p. 51-55.
[15] Lawn, B.R., *Fracture of brittle solids*. 1993: Cambridge university press.
[16] Maazouz, Y., et al., *Robocasting of biomimetic hydroxyapatite scaffolds using self-setting inks.* Journal of Materials Chemistry B, 2014. **2**(33): p. 5378-5386.
[17] Miranda, P., et al., *Mechanical properties of calcium phosphate scaffolds fabricated by robocasting.* Journal of Biomedical Materials Research Part A, 2008. **85A**(1): p. 218-227.